

Surface EXAFS *via* differential electron yield

Noritake Isomura,^{a*} Takaaki Murai,^b Toyokazu Nomoto^b and Yasuji Kimoto^a

^aToyota Central R&D Labs Inc., 41-1 Yokomichi, Nagakute, Aichi 480-1192, Japan, and

^bAichi Synchrotron Radiation Center, 250-3 Minamiyamaguchi-cho, Seto, Aichi 489-0965, Japan.

*Correspondence e-mail: isomura@mosk.tytlabs.co.jp

Received 1 November 2016

Accepted 8 December 2016

Edited by S. M. Heald, Argonne National Laboratory, USA

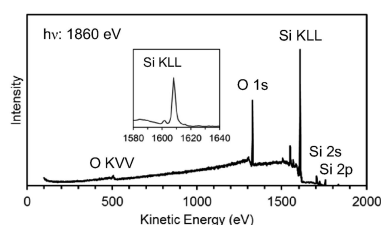
Keywords: XAS; EXAFS; silicon dioxide; partial electron yield; surface-sensitive.

Surface-sensitive analysis *via* extended X-ray absorption fine-structure (EXAFS) spectroscopy is demonstrated using a thickness-defined SiO₂ (12.4 nm)/Si sample. The proposed method exploits the differential electron yield (DEY) method wherein Auger electrons escaping from a sample surface are detected by an electron analyzer. The DEY method removes local intensity changes in the EXAFS spectra caused by photoelectrons crossing the Auger peak during X-ray energy sweeps, enabling EXAFS analysis through Fourier transformation of wide-energy-range spectral oscillations. The Si *K*-edge DEY X-ray absorption near-edge structure (XANES) spectrum appears to comprise high amounts of SiO₂ and low Si content, suggesting an analysis depth, as expressed using the inelastic mean free path of electrons in general electron spectroscopy, of approximately 4.2 nm. The first nearest neighbor (Si–O) distance derived from the Fourier transform of the Si *K*-edge DEY-EXAFS oscillation is 1.63 Å. This value is within the reported values of bulk SiO₂, showing that DEY can be used to detect a surface layer of 12.4 nm thickness with an analysis depth of approximately 4.2 nm and enable ‘surface EXAFS’ analysis using Fourier transformation.

1. Introduction

X-ray absorption spectroscopy (XAS) is increasingly required for the surface analysis of materials because it provides information on not only chemical states but also on local atomic structures, which cannot be obtained through general surface analysis methods such as X-ray photoelectron spectroscopy (XPS) or Auger electron spectroscopy. A particular type of XAS, extended X-ray absorption fine structure (EXAFS) spectroscopy, with Fourier transformation of the spectral oscillations, can be used to determine interatomic distances and coordination numbers (Teo & Joy, 1980). However, EXAFS has rarely been applied for surface analysis with an analysis depth of a few nanometers.

Partial electron yield (PEY), which is used to detect electrons escaping from material surfaces, has been proposed as a surface-sensitive method (Brennan *et al.*, 1981; Stöhr, 1979; Nakanishi & Ohta, 2012). One particular method for detecting Auger electrons with elemental-specific energy is called Auger electron yield (AEY) (Citrin *et al.*, 1978; Brennan *et al.*, 1981). However, simultaneously produced photoelectrons undergo changes in their energy during an energy sweep of incident X-rays. Hence, the photoelectron peaks often cross the Auger peaks at fixed energies, causing local intensity changes in the XAS spectra. These local changes are a critical problem for EXAFS, which requires a wide-energy-range spectrum of more than 400 eV. Stöhr (1979) proposed a method to avoid photoelectron crossing by detecting secondary electrons with



low energy. However, these secondary electrons, which are electrons that have lost energy in the solid bulk, originate primarily from Auger electrons, suggesting a greater depth than the AEY (Isomura *et al.*, 2015). In most cases, PEY measurement is performed using X-ray absorption near-edge structure (XANES) spectroscopy, which does not require a wide-energy-range spectrum and is analyzed by comparison with the spectra of standard materials. In the case of XANES, measurements of low absorption energy such as the *L*-edge are more surface sensitive than those of *K*-edges even in total electron yield (TEY) (Kasrai *et al.*, 1996).

We previously reported on the differential electron yield (DEY) method, one of the PEY methods that can avoid photoelectron crossing (Isomura *et al.*, 2016). DEY can be surface sensitive because it detects Auger electrons. However, the study only showed that DEY could be used to perform EXAFS analysis using Fourier transformation of the spectral oscillations, and the analysis depth was not confirmed because a bulk sample was used. In this study, the surface-sensitive performance of the DEY-EXAFS method is demonstrated using a thickness-defined sample (SiO₂/Si).

2. Experimental

The experiments were performed at the soft X-ray XAS beamline BL6N1 of the Aichi Synchrotron Radiation Center (AichiSR) (Yamamoto *et al.*, 2014; Isomura *et al.*, 2015), which has an electron storage ring with a circumference of 72 m and is operated at an electron energy of 1.2 GeV with a current of 300 mA. White light from a bending magnet was monochromated by an InSb(111) double-crystal monochromator. The beam size at the sample position was approximately 2 mm (horizontal) × 1 mm (vertical). The horizontal size of the irradiated region of the sample surface depended on the sample tilt.

The electron analyzer (PHOIBOS 150, SPECS GmbH) can operate over a range of kinetic energies (from 1 to 3500 eV). It comprises a hemispherical energy analyzer with a mean radius of 150 mm, a pre-retarding combined second-order focusing-lens system, and a two-dimensional event-counting detector equipped with a multichannel plate, a phosphor screen and a charge-coupled device camera. In the experiments, the pass energy was 10 eV and total energy resolution $E/\Delta E$ was approximately 2500. The X-ray beam from the beamline was horizontally incident and horizontally polarized. The axis of the input lens of the analyzer (acceptance angle = $\pm 5^\circ$) was on the horizontal plane and the angle between the axis and the incident beam was 54° . The take-off angle of the analyzed electrons was set to 90° (normal to the surface). In the DEY measurements, electrons emitted from the sample surface were detected by the electron analyzer during X-ray energy sweeps. In the TEY measurements performed for comparison, a sample drain current was measured. The base pressure of the main chamber was approximately 5×10^{-8} Pa.

The sample structure was a SiO₂ (12.4 nm)/Si(111) film formed by thermal oxidation of Si. The film thickness was measured by an ellipsometer (L115C, Gaertner Scientific Co.).

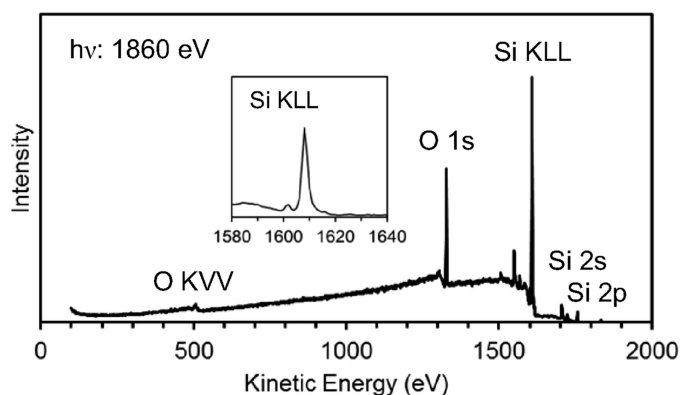


Figure 1
X-ray photoelectron spectroscopy spectrum of the SiO₂/Si sample surface at a photon energy of 1860 eV. The inset shows an enlarged view of Si *KLL*.

3. Results and discussion

Fig. 1 shows the XPS spectrum of the SiO₂/Si sample surface under irradiation at a photon energy of 1860 eV. In the spectrum, the Auger and photoelectron peaks that can be assigned to Si and O contained in the sample are observed. The Auger peak at 1608 eV is assigned to Si *KLL* (Johansson *et al.*, 2003). The Auger and background intensities were monitored at electron energies of 1608 and 1628 eV, respectively, during the X-ray energy sweeps as part of the two types of EXAFS measurements (hereafter ‘Auger EXAFS’ and ‘background EXAFS’, respectively). The electron energy for the background EXAFS should be set as far from the Si *KLL* peak as possible to avoid the overlap. However, the energy difference between the Auger and background should be small because those energies should essentially be the same, and was set to 20 eV in consideration of the Si *KLL* peak tail.

The Auger and background EXAFS spectra are shown in Fig. 2. The Auger and background intensities are normalized by the incident X-ray intensities determined using the current of an Al mesh inserted into the path of the X-ray beam. The

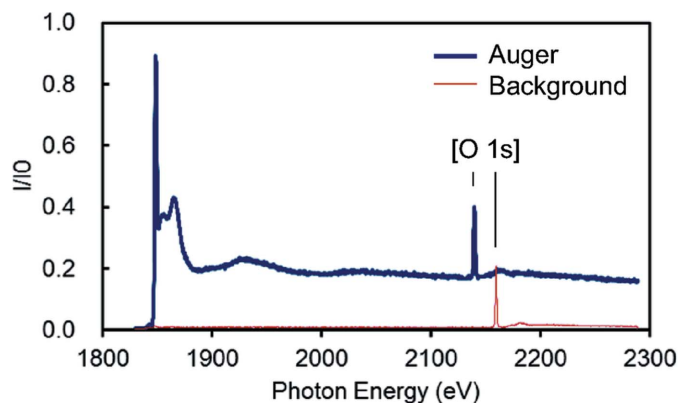


Figure 2
Si *K*-edge extended X-ray absorption fine structure (EXAFS) spectra measured at different Si *KLL*: Auger peak (1608 eV) and background peak (1628 eV), indicated as blue and red lines, respectively. The brackets indicate the peak caused by photoelectron crossing electron energy windows for the Auger and background spectra.

Auger EXAFS spectrum corresponds to the AEY spectrum. As can be observed in Fig. 2, the Si *K*-edge is seen at 1850 eV in the Auger EXAFS spectrum but not in the background spectrum. The local intensity increase at 2140 eV is caused by the O 1s photoelectron crossing in the Auger EXAFS spectrum. A hill-like increase at the higher peak energy is caused by crossing of the energy-loss spectral shape of the O 1s photoelectrons with inelastic scattering in the solid. In general, EXAFS analysis using Fourier transformation requires at least 400 eV ranging from the absorption edge. These increases, which are caused by the photoelectrons, disable EXAFS analysis because they disturb the analyzed small spectral oscillations. However, the increases are also observed in the background EXAFS spectrum, although at different energies from the Auger EXAFS spectrum.

The positions of the increases in the background EXAFS spectrum are shifted toward higher energies (by 20 eV) than those in the Auger EXAFS spectrum because the monitoring energy for the background was placed at an electron energy that was 20 eV higher than that of the Auger energy and the photoelectron peaks crossed each monitoring energy at photon energies that differed from each other by 20 eV. The DEY-EXAFS spectrum, which is shown in Fig. 3, was obtained following subtraction of the background spectrum from the Auger EXAFS spectrum. This subtraction was performed after down-shifting the energy level of the background EXAFS spectrum by 20 eV, following the procedure for DEY-EXAFS analysis (Isomura *et al.*, 2016). The increases caused by the O 1s photoelectrons and energy-loss shape are both removed in the DEY-EXAFS spectrum. In addition to the Si *K*-edge at 1850 eV, local maxima appear in the DEY-EXAFS spectrum at 1930, 2050 and 2170 eV, likely as a result of EXAFS oscillations.

The XANES spectrum of DEY is shown in Fig. 4, along with that of TEY with an analysis depth of a few tens of nanometers in the Si *K*-edge (Nakanishi & Ohta, 2012) for comparison. In the TEY spectrum, peaks are observed at 1842 and 1848 eV, which are assigned to Si and SiO₂, respectively (Nakanishi & Ohta, 2012). On the other hand, the DEY spectrum seems to comprise high amounts of SiO₂ and low Si content. The inelastic mean free path (IMFP) of electrons in

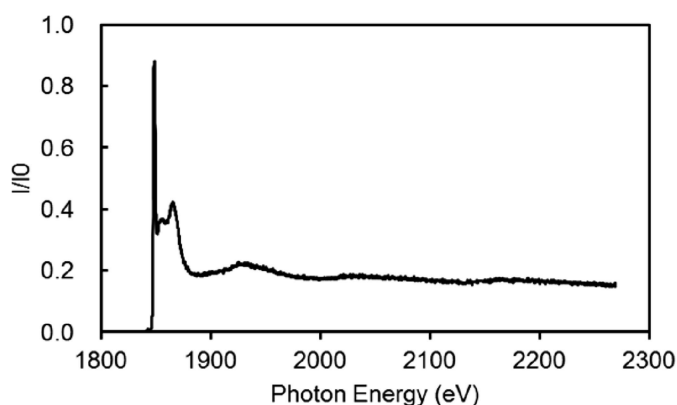


Figure 3
Differential electron yield (DEY)-EXAFS spectrum for the Si *K*-edge.

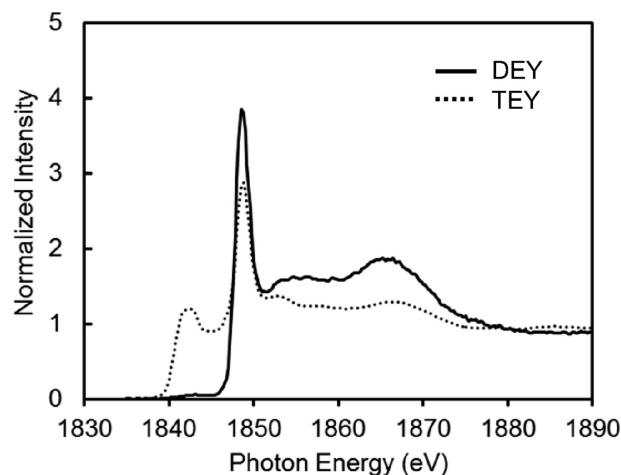


Figure 4
X-ray absorption near-edge structure spectra for the Si *K*-edge. The solid and dotted lines indicate DEY and TEY, respectively.

SiO₂ is estimated to be 4.2 nm at a kinetic energy of 1608 eV, calculated using the TPP-2M formula (Tanuma *et al.*, 1994). Ninety-five percent of the total signal originates from three times the depth of IMFP (Bare *et al.*, 2016), which is called the ‘information depth’ of XPS and is calculated to be 12.6 nm. This value is in close agreement with or slightly more than the SiO₂ thickness of 12.4 nm and is consistent with the above-mentioned result that the DEY spectrum comprises high amounts of SiO₂ and low amounts of Si. Conversely, it translates to an analysis depth, expressed using the IMFP in general electron spectroscopy, of approximately 4.2 nm for the Si *K*-edge of SiO₂. For comparison, the analysis depth of TEY seems to be 25–30 nm, which is the SiO₂ film thickness for which the substrate intensity is reduced to 1/e (approximately 37%) for SiO₂/Si (Nakanishi & Ohta, 2012).

Fig. 5 shows the oscillation as a function of wavevector extracted from the DEY-EXAFS spectrum shown in Fig. 3 using the *ATHENA* program (Ravel & Newville, 2005). The Fourier transform for an oscillation range of $k = 3\text{--}10 \text{ \AA}^{-1}$ (without considering the phase shifts) derived from the oscillation is shown in Fig. 6. The spike noise at 8.65 \AA^{-1} can be seen in Fig. 5. This was caused by a small mismatch of data points between the Auger and background, because the subtraction of those spectra with a steep fluctuation due to the photoelectron crossing was performed. However, the local peak in the EXAFS oscillation generally has little influence on the derived Fourier transform. The first nearest neighbor distance was calculated *via* a fitting analysis using the *ARTEMIS* program (Ravel & Newville, 2005), and the phase shift and backward scattering factor values were calculated *via* *FEFF* (Zabinsky *et al.*, 1995; Ankudinov *et al.*, 1998). The parameters used included the atomic distance, amplitude and edge energy whereas the Debye–Waller factor was fixed. The amplitude reduction factor was set to 1.021, determined from the TEY-EXAFS of bulk SiO₂. The obtained Si–O distance was 1.63 Å with a reliability factor of 0.02. Barranco *et al.* (2001), Kamijo *et al.* (1996) and Gritsenko (2008) reported Si–O distances of 1.66, 1.64 and 1.62 Å, respectively. It is

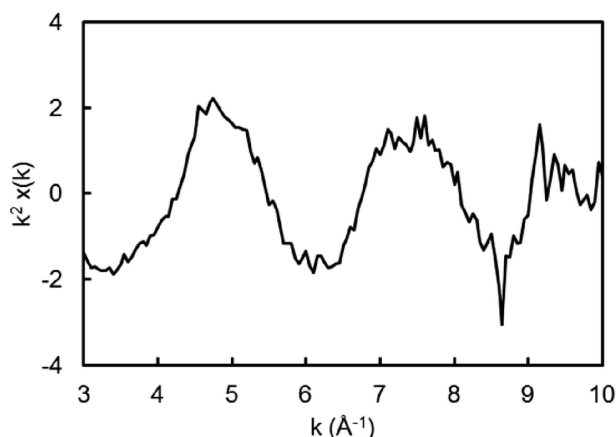


Figure 5
EXAFS oscillation for the Si *K*-edge as a function of wavevectors from Fig. 3.

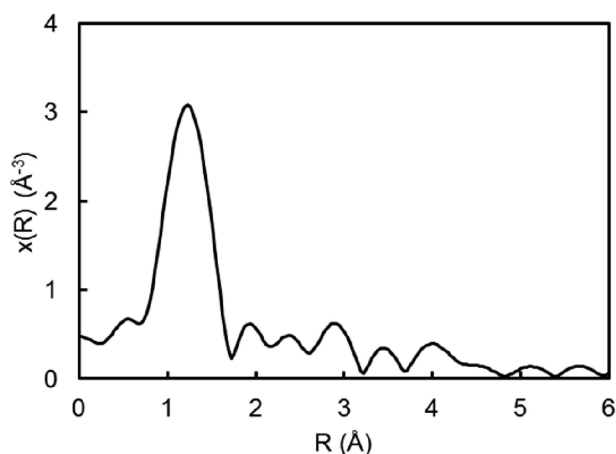


Figure 6
Fourier transform derived from EXAFS oscillation for the Si *K*-edge without considering the phase shifts.

believed that these values vary because SiO₂ has various crystal structures such as quartz and cristobalite. Our result was within these reported values, showing that the DEY method can detect a 12.4 nm-thick surface layer with an analysis depth of approximately 4.2 nm and, unlike XANES analysis, which relies on comparison with spectra of standard samples, allows for ‘surface EXAFS’ analysis using Fourier transformation. In addition, this method does not require a sample with very smooth surface essentially, as detected at the surface normal, which is contrasted with the method detecting fluorescent X-rays or electrons at grazing angles for surface-sensitive measurements (Shinoda *et al.*, 2010; Amemiya *et al.*, 2003).

4. Conclusions

A surface-sensitive EXAFS analysis exploiting the DEY method was demonstrated using a thickness-defined SiO₂ (12.4 nm)/Si sample. The Si *K*-edge DEY-XANES spectrum appears to comprise a high amount of SiO₂ and low

amounts of Si, suggesting an analysis depth, expressed using the IMFP in general electron spectroscopy, of approximately 4.2 nm. The first nearest neighbor (Si–O) distance derived from a Fourier transform of the Si *K*-edge DEY-EXAFS oscillation was 1.63 Å, which is within the reported values of SiO₂. This result shows that DEY can detect a surface layer of 12.4 nm thickness with an analysis depth of approximately 4.2 nm and allows for EXAFS analysis through Fourier transformation. We expect that this ‘surface EXAFS’ method will become a useful tool for surface analysis.

Acknowledgements

The authors are grateful to Dr Masao Kamada, Saga University, who co-developed the DEY-EXAFS method used in this study. The authors thank Dr Takamasa Nonaka, Toyota Central R&D Labs Inc., for his advice. Synchrotron radiation measurements were performed at BL6N1 of AichiSR, Aichi Science and Technology Foundation (Experimental No. 201502022).

References

- Amemiya, K., Kitagawa, S., Matsumura, D., Yokoyama, T. & Ohta, T. (2003). *J. Phys. Condens. Matter*, **15**, S561–S571.
- Ankudinov, A. L., Ravel, B., Rehr, J. J. & Conradson, S. D. (1998). *Phys. Rev. B*, **58**, 7565–7576.
- Bare, S. R., Knop-Gericke, A., Teschner, D., Hävacker, M., Blume, R., Rocha, T., Schlögl, R. A., Chan, S. Y., Blackwell, N., Charochak, M. E., ter Veen, R. & Brongersma, H. H. (2016). *Surf. Sci.* **648**, 376–382.
- Barranco, A., Mejías, J. A., Espinós, J. P., Caballero, A., González-Elipe, A. R. & Yubero, F. (2001). *J. Vac. Sci. Technol. A*, **19**, 136–144.
- Brennan, S., Stöhr, J. & Jaeger, R. (1981). *Phys. Rev. B*, **24**, 4871–4874.
- Citrin, P. H., Eisenberger, P. & Hewitt, R. C. (1978). *Phys. Rev. Lett.* **41**, 309–312.
- Gritsenko, V. A. (2008). *Phys. Usp.* **51**, 699.
- Isomura, N., Kamada, M., Nonaka, T., Nakamura, E., Takano, T., Sugiyama, H. & Kimoto, Y. (2016). *J. Synchrotron Rad.* **23**, 281–285.
- Isomura, N., Soejima, N., Iwasaki, S., Nomoto, T., Murai, T. & Kimoto, Y. (2015). *Appl. Surf. Sci.* **355**, 268–271.
- Johansson, L. I., Virojanadara, C., Eickhoff, Th. & Drube, W. (2003). *Surf. Sci.* **529**, 515–526.
- Kamijo, N., Handa, K. & Umesaki, N. (1996). *Mater. Trans. JIM*, **37**, 927–931.
- Kasrai, M., Lennard, W. N., Brunner, R. W., Bancroft, G. M., Bardwell, J. A. & Tan, K. H. (1996). *Appl. Surf. Sci.* **99**, 303–312.
- Nakanishi, K. & Ohta, T. (2012). *Surf. Interface Anal.* **44**, 784–788.
- Ravel, B. & Newville, M. (2005). *J. Synchrotron Rad.* **12**, 537–541.
- Shinoda, K., Suzuki, S., Yashiro, K., Mizusaki, J., Uruga, T., Tanida, H., Toyokawa, H., Terada, Y. & Takagaki, M. (2010). *Surf. Interface Anal.* **42**, 1650–1654.
- Stöhr, J. (1979). *J. Vac. Sci. Technol.* **16**, 37.
- Tanuma, S., Powell, C. J. & Penn, D. R. (1994). *Surf. Interface Anal.* **21**, 165–176.
- Teo, B. K. & Joy, D. C. (1980). *EXAFS Spectroscopy*. New York: Plenum.
- Yamamoto, M., Yoshida, T., Yamamoto, N., Yoshida, H. & Yagi, S. (2014). *e-J. Surf. Sci. Nanotech.* **12**, 299–303.
- Zabinsky, S. I., Rehr, J. J., Ankudinov, A., Albers, R. C. & Eller, M. (1995). *Phys. Rev. B*, **52**, 2995–3009.